



Sustainable
Energy & Fuels

**Carbon Capture from Corn Stover Ethanol Production via
Mature Consolidated Bioprocessing Enables Large Negative
Biorefinery GHG emissions and Fossil Fuel-Competitive
Economics**

Journal:	<i>Sustainable Energy & Fuels</i>
Manuscript ID	SE-ART-03-2023-000353.R2
Article Type:	Paper
Date Submitted by the Author:	28-Apr-2023
Complete List of Authors:	Kubis, Matthew; Thayer School of Engineering at Dartmouth, Lynd, Lee; Thayer School of Engineering at Dartmouth,

SCHOLARONE™
Manuscripts

ARTICLE

Carbon Capture from Corn Stover Ethanol Production via Mature Consolidated Bioprocessing Enables Large Negative Biorefinery GHG emissions and Fossil Fuel-Competitive Economics

Received 00th January 20xx,
Accepted 00th January 20xx

DOI: 10.1039/x0xx00000x

Matthew R. Kubis^{a,b}, Lee R. Lynd^{a,b,*}

Process simulation and techno-economic analysis was used to evaluate corn stover conversion to ethanol via mature consolidated bioprocessing and cotreatment (C-CBP) technology with carbon capture and storage (CCS). Process design was explored pursuant to increasing energy efficiency and greenhouse gas (GHG) emission reductions for a 60 million gallon per year facility featuring coproduction of fuel pellets, electricity, CO₂, and renewable natural gas (RNG) in various combinations. After performing heat integration for C-CBP, process heat was able to be met entirely from onsite biogas production and without any solid process residue combustion. When compared to its reference case, incorporating high-purity CCS and biogas upgrading led to a 4.3-fold improvement in net negative biorefinery GHG emissions (-85 gCO₂eq/MJ ethanol) while also lowering the minimum ethanol selling price (MESP). Recovering CO₂ from high-purity streams had a levelized cost of capture estimated between 14 to 15 \$/ton CO₂, well below current estimates for lowest-cost capture systems projected at fossil energy plants. Cellulosic ethanol production via C-CBP with high-purity CCS was generally cost-competitive with wholesale gasoline prices on an energy equivalent basis. Total carbon capture, including all potential emissions from onsite flue gas and fuel pellet coproduct combustion in addition to high-purity streams, led to net negative biorefinery GHG emissions of -170 to -154 gCO₂eq/MJ ethanol. Because C-CBP remains configurationally distinct from other biological conversion pathways with thermochemical pretreatment and added fungal cellulase, it enables a dramatically lower cost of production while simultaneously achieving negative carbon emissions. To our knowledge, this is the first analysis of CCS for cellulosic ethanol produced by routes not involving thermochemical pretreatment and added enzymes, and the GHG mitigation potential values reported here are the highest to date for cellulosic ethanol with CCS.

Introduction

Primary energy annually supplied by non-traditional biomass energy systems is projected to expand 5-fold (from 25 to 128 EJ) by 2060 to meet climate stabilization objectives (1). Use of inedible cellulosic biomass is generally recognized as a priority in light of large potential supply, decreased competition for food resources, and lower GHG emissions compared to edible biomass feedstocks (2). Corn stover is a residue of corn grain production consisting of stalks, cobs, and husks, one of the most abundant cellulosic biomass resources in the United States, and is projected to play a central role in emergent cellulosic biofuel deployment (3–5). Among biologically derived fuels or fuel intermediates, ethanol distinctively combines desired features including high yield and titer, ease of separation, anaerobic production, and can be used as a fuel or as an intermediate for synthesis of higher molecular weight hydrocarbon fuels (6–8).

Determining the climate change mitigation potential of bioethanol is most often approached using a well-to-wheels life-cycle analysis in terms of CO₂ equivalent emissions per MJ

ethanol (9–11). Net life-cycle emissions result from the sum of positive and negative emission contributions in the supply chain, biorefinery, and coproduct utilization. Positive contributions are typically feedstock production and transport, product distribution, and biorefinery emissions associated with process energy and chemical inputs. Biorefinery emissions are the largest contributor to emissions in most studies, with chemical inputs being on the order of a third of total biorefinery emissions (9,10). Land use change for corn stover production has been estimated at -0.7 gCO₂eq/MJ ethanol, corresponding to <1% of a gasoline base case (12). Net emissions are decreased as a result of avoided fossil fuel emissions (AFFE) via coproducts such as electricity generated from lignin-rich solid process residues. The chemical combustion of bioethanol is usually considered to be carbon neutral (9).

Industrial-scale conversion of corn stover to ethanol via fermentation has been studied in a variety of configurations summarized in appendix A.1. Many studies involve thermochemical dilute-acid pretreatment with added fungal cellulase, with widely cited studies by the National Renewable Energy Laboratory (NREL) providing detailed design and cost estimation (3,13–16). Alternative, less-developed processing innovations with potential for lower costs and emissions continue to be investigated (17–19). One alternative is consolidated bioprocessing (CBP) with mechanical disruption during fermentation (cotreatment) in lieu of thermochemical pretreatment (20), thereby avoiding emissions and costs

^a Thayer School of Engineering, Dartmouth College, 14 Engineering Drive, Hanover, NH 03755 USA.

^b The Center for Bioenergy Innovation, Oak Ridge National Laboratory, Oak Ridge, TN 37831 USA.

*Correspondence: Lee.R.Lynd@Dartmouth.edu

Electronic Supplementary Information (ESI) available at DOI: 10.1039/x0xx00000x

related to chemical inputs and enzyme production. In this direction, Lynd et al. (2017) analyzed production via C-CBP with projected bioconversion efficiencies enabled by future research and development (20). This scenario eliminated thermochemical pretreatment as well as added cellulase, substituted a gas boiler for a solids boiler, and converted solid process residues into a fuel pellet coproduct rather than being burned on-site to generate electricity. As a result of lowering capital investment and increasing coproduct revenue, the authors report significantly reduced payback periods and improved GHG emission reductions per ton feedstock compared to a base-case featuring thermochemical pretreatment and added fungal cellulase.

Published assessments of GHG mitigation with biofuels have focused primarily on displaced fossil fuel emissions rather than CO₂ capture (21,22). It has been suggested that in time the value of biomass energy systems for photosynthetic carbon removal may exceed that for energy supply (23,24). Studies have recently begun to leverage carbon capture and storage (CCS) technologies to enable net negative life-cycle emissions for biofuel production (11,25–27). Yang et al. (2020) demonstrated net negative life-cycle emissions for cellulosic sorghum ethanol at -21.3 and -109 gCO₂eq/MJ ethanol for recovery of high purity CO₂ and all CO₂ emitted, respectively. In Kim et al (2020), CCS from all production emissions improved the average life cycle GHG mitigation from 67.2 to -43.8 gCO₂eq/MJ. Gelfand et al., (2020) focused primarily on impact of biomass supply chain on soil carbon stocks and report that corn stover ethanol emission intensity improved from 19.8 to -98.7 gCO₂eq/MJ with CCS inclusion. Geissler and Maravelias (2021) have also shown CCS to enable net negative GHG emissions, e.g., from 24.7 to -22.6 gCO₂eq/MJ and only capture from fermentation was required to achieve net negative emissions. All analyses known to us of CCS applied towards cellulosic ethanol were based on processes featuring thermochemical pretreatment and added enzymes.

Commercial bioethanol production is a logical starting point technologies because of high-purity CO₂ streams (produced via fermentation or anaerobic digestion) compared to more-dilute onsite flue gas. It has been reported that the levelized cost of CO₂ capture scales inversely with concentration (28). The cost of separating CO₂ from dilute flue gas (< 20% CO₂) is projected to be between \$30-\$70/ton before compression can be performed (26,28–33), whereas during ethanol fermentation, nearly pure CO₂ is generated as a saturated gas at low to atmospheric pressure (34). Largely related to separation costs, capturing CO₂ from combustion diluted flue gas requires around 10-fold more energy than from fermentation sources (26). Onsite biogas, an intermediate stream generated during anaerobic digestion (AD) of thin stillage, consists of roughly 50/50 (v/v) CH₄ and CO₂. Biogas upgrading via membrane separation is a promising technology that can deliver high-purity streams of both methane (i.e., renewable natural gas or RNG) and CO₂ (25,35,36). Collectively, the total levelized cost of sequestration for high-purity and dilute flue gas sources are generally around \$30-50/t CO₂ and \$70-\$120/t CO₂, respectively (25,30,33,37,38).

To date, there have been numerous studies investigating the CCS potential at fossil energy plants (32,33,39), industrial sectors (28,30,40), and corn ethanol production (30,34,37,41–45). Prior studies of CCS applied to cellulosic biofuel production have been limited to processes involving thermochemical

pretreatment and added fungal cellulase (27,46–48). A knowledge gap thus exists with respect to evaluating the CCS potential of other process concepts, which we address here for C-CBP. Specifically, we present an updated techno-economic evaluation of corn stover ethanol via C-CBP aimed at increasing energy efficiency and leveraging alternative coproduction strategies including CCS for revenue and climate stabilization benefits. Minimum ethanol selling price (MESP) and net biorefinery GHG emission reductions are evaluated and presented.

Methodology

Scenario Definitions and Methods

This study builds on the previous report of Lynd et al. (2017) that described the performance and cost of a simulated cellulosic ethanol biorefinery featuring C-CBP intended to represent long-term potential (20). Material and energy flows were modeled using ASPEN PLUS[™] (V10) process simulations and economic analyses were adapted from the NREL study of corn stover-to-ethanol by Humbird et al. (2011). In the updated techno-economic analysis presented here, changes were made to the process simulation without changing major conversion parameters related to ethanol bioconversion efficiency, e.g., solid loading (19.5 wt.%), carbohydrate solubilization (88%), fermentation yield (0.46 g/g solubilized carbohydrate or 85.6 gallons per dry metric ton feedstock), and ethanol throughput (60 million gallon per year). A summary table of fermentation conditions and conversion parameters is available in appendix A.2.

New scenarios were analyzed stepwise incorporating the following design features: 1) enhanced heat integration, 2) biogas surplus to electricity generation using a gas turbine, 3) fermentation-CO₂ capture for carbon capture and storage, 4) biogas membrane upgrading with biogas-CO₂ capture and surplus RNG sales and lastly, 5) an RNG turbine to generate electricity instead of selling surplus RNG. These scenarios were evaluated with respect to greenhouse gas emissions, minimum ethanol selling prices (MESPs), and CO₂ levelized costs of capture. A summary description of scenario inputs, outputs, and GHG benefits are presented in appendix A.5. Technical details regarding the scenario modifications are described in the sections immediately below.

Scenario I – Enhanced Heat Recovery

Increasing the operating pressure of the distillation train (both the beer and rectification columns) from 1 to 3.2 atm was implemented to recover the latent heat in overhead vapor condensation via heat exchange and generated saturated steam to inject during feedstock pasteurization. In the advanced case described in Lynd et al. (2017), referred to herein as the reference case, process steam supplied the heat duty both to distillation (38.5 MMkcal/hr) and feedstock pasteurization (23.4 MMkcal/hr) while a distillation-related heat duty of similar magnitude (-20.3 MMkcal/hr) was lost to the ambient environment by an air-cooled rectification column condenser. Redirecting the air-cooled condenser duty for pasteurization was the

primary source of heat recovery in this study. A Summary diagram for enhancing recovery is depicted below in Figure 1.

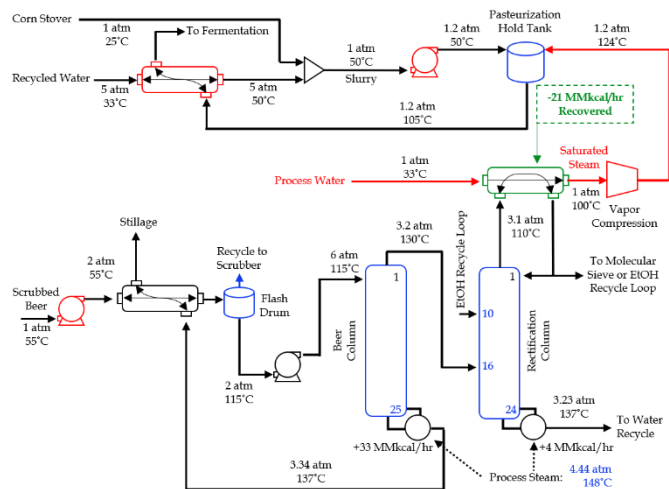


Figure 1. Heat recovery diagram. Modifications made to the existing equipment are depicted in blue and newly installed equipment in red. Exchanging the air-cooled condenser with a shell-and-tube heat exchanger (in green) enabled low-grade steam generation which was compressed and injected for pasteurization. Distillation operating pressure was increased from 1 to 3.2 atm to enable waste heat recovery.

In the revised beer column, the overhead vapor condenser was omitted with wet ethanol vapor leaving the top stage instead of a vapor side draw, resulting in a conventional stripping column. A pump discharging the beer stream at 2 atm was added to the upstream scrubber recycling loop to promote CO₂ separation prior to distillation. The beer stream was then preheated to 114°C using a beer stillage economizer, and an adiabatic vapor-liquid separation at 2 atm and 114°C was performed to recycle CO₂ back to the water scrubber. The CO₂ removal by the upstream scrubber/recycle loop was > 99.9%, with less CO₂ remaining in the distillation feed than in the Humbird et al. design (3). Ethanol leaving in the bottoms was fixed at 0.05% mass fraction by varying reboiler duty. The operating pressure was set at 3.2 atm, and the stage number was increased from 16 to 25. In the revised rectifying column: operating pressure was also increased to 3.1 atm, and the stage number was reduced from 35 to 24. A pressure drop of 0.006 atm per stage was assumed. Across both columns, the total number of stages was kept constant relative to the reference case, though stages were moved from the rectification column to the beer column. In the revised rectification column, the feed stages for the wet ethanol vapor and molecular sieve recycle loop were set to stages 16 and 10, respectively. Ethanol leaving in the bottoms was fixed at 0.05% mass fraction by varying the distillate rate. The ethanol-rich vapor was fixed at 92.5% mass fraction by varying the reflux ratio. In both columns, stage number and feed stages were decided heuristically based on separation performance and heat demand. The low-pressure saturated steam was compressed (75% isentropic efficiency) to 1.2 atm and 124°C to inject into pasteurization. Saturated process steam (generated via the gas boiler) was changed from 2.1 to 4.44 atm to fire the distillation columns at elevated pressure (3.2 atm).

The pasteurization procedure was revised to reflect anticipated operating conditions of a cellulosic ethanol facility. Holding of the unfermented corn stover slurry was changed from 100°C & 1 atm for

an hour in the reference case to 105°C & 1.2 atm for thirty minutes in the revised scenarios (I-V). An additional pump discharging the slurry at 1.2 atm was used to feed the pasteurization tank. Injection of the steam generated by condensing distillation vapor as described above was the primary supply of heat; however, it became necessary to feed the recycled water at 50°C instead of 33°C to reach pasteurization temperature. A spiral plate heat exchanger was included to recycle heat from the hot stream leaving pasteurization (105°C), and roughly a quarter of available heat remaining in the pasteurized, hot corn stover slurry was used in feed water preheating (33° to 50°C) with the remaining heat duty chilled by the cooling tower.

The purchase cost for the distillation train at elevated pressure was adapted from Humbird et al. (2011), as the original cost estimate was designed for an operating pressure of 2 atm and the pressure cost factor is not expected to change significantly from 2 atm to 3.2 atm (47). Some equipment changes were made to reflect the new design. The purchase cost for a beer column condenser was deducted, and the purchase cost for the air-cooled condenser was replaced with a water-cooled shell-and-tube condenser. A compressor was added for mechanical steam compression. For pasteurization, an additional pump and spiral plate heat exchanger was included and the capital cost for the tank was calculated using the revised hold time. A summary of all revised capital equipment purchase costs can be found in appendix B.

Scenario II – Biogas Electricity Generation

Partial on-site electricity production was investigated to realize value from the excess biogas made available by the enhanced heat integration strategy described above. Biogas turbine systems operate similarly to their natural gas turbine counterparts except for the presence of CO₂ in the fuel stream (49–51). Comparing gas and biogas turbines, it has been previously reported that biogas turbines demonstrate higher heat recovery and turbine efficiency, but overall lower net efficiency due to power requirements in fuel compression. However, the net power output is nearly constant regardless of fuel composition after accounting for fuel compression and overall performance is not expected to differ significantly (50,51).

Gas turbine performance parameters were adapted from the literature as specified in appendix A.3 (36,51–53). Heat recovery from turbine exhaust is common in combined cycle gas turbine platforms, and heat-to-process-steam was implemented here rather than generating additional electricity via steam turbines. Hot turbine exhaust (675–698°C) was used to partially vaporize process condensate (148°C) from distillation in a spiral plate heat exchanger using a hot/cold outlet temperature approach of 10 °C, and the cooled exhaust (158°C) was vented to the environment. Capital cost estimation for the turbine and heat exchanger are available in appendix B. An iron-oxide sponge for biogas desulphurization was adapted from Abatzoflou and Boivin (2008) but not expressly simulated (54). Capital costs for desulphurization equipment were also applied to the reference case.

Scenario III- Biogas Electricity & Fermentation CCS

Design parameters and capital costs for on-site CO₂ compression were adapted from the NETL technical report *Cost of Capturing CO₂ from Industrial Sources (2014) DOE/NETL-2013/1602*. A reciprocating

compressor delivers fermentation CO₂ at 15.3 MPa and 49°C, conditions suitable for pipeline transportation (28,30). Pipeline instead of truck transport was assumed to be more cost effective considering the annual estimated CO₂ production would be well above >0.1 million tons of CO₂ per year, i.e., an approximate cut-off for truck transport (28).

Interstage cooling and dehydration was simulated to reduce water content in the CO₂ stream (28,55). In the reference case, fermentation off-gas underwent water-scrubbing to capture any volatilized ethanol which results in a CO₂ stream with 2.4% water content by mass, above the specified conditions for transport: 50–840 ppmv (29). A five-stage compressor with interstage cooling was simulated where low pressure CO₂ (0.101 MPa) was first compressed to moderate pressure (3.8 MPa) using three stages, cooled to 28°C for vapor-liquid separation and compressed to high pressure (15.3 MPa) using the remaining two stages (55). Vapor-liquid separation flash drums were intended to simulate various interstage coolers and knockout vessels used to decrease temperature and remove moisture. High pressure CO₂ was cooled to 49°C for vapor-liquid separation removing a cumulative of 98.8% of H₂O and leaves the CO₂ stream with 74 ppmv water content at 15.3 MPa. The electricity demand for CO₂ compression was determined in ASPEN using compressor isentropic and mechanical efficiencies of 88% and 99%, respectively.

Scenario IV – RNG & High-Purity CCS

Biogas upgrading via membrane separation into renewable natural gas (RNG) which was assumed necessary to sell surplus biogas/methane generated as described in Scenario I. Biogas upgrading performance parameters were adapted from Deng and Hägg (2010) to purify CO₂ and upgrade CH₄ in a 2-stage configuration with symmetric cascade recycling using polyvinylamine/polyvinylalcohol (PVAm/PVA) blend membranes and are recapitulated in appendix A.4. Capital costs were also adapted, and electricity demand was determined using ASPEN simulations. The module lifetime was increased from 20 to 30 years by including two additional hollow fiber membranes each with a 5-year lifetime. Equipment cost estimates were scaled in proportion to the biogas feed rate (Table 2, shown in brackets). Compressors were sized using a six-tenths exponent (Humbird et al., 2011) and membrane modules were scaled linearly. Capital costs are presented in appendix B.

Scenario V – RNG Electricity and High-Purity CCS

The biogas turbine from scenario II was placed downstream from the biogas upgrading described in scenario IV. As with surplus biogas, only a fraction of the total RNG (i.e., the surplus) was routed to the turbine (approximately 38%) whereas the remainder was combusted specifically for process heat. Because RNG is delivered from the biogas membrane upgrading module at 20 bar, no additional fuel compression is required for gas turbine operation, which improved the modular thermal efficiency relative to firing-biogas (appendix A.3).

Solids Combustion, Electricity Generation, and Flue Gas Capture

The following adjustments were made to Scenario V to study the differences between fuel pellet and electricity coproduction regarding MESP and GHG reductions. Fuel pellets revenue, capital

expense, and electricity consumption were removed from project economics. The gas boiler (2.5 MM\$) was replaced with a solids boiler (46.2 MM\$), and a 42.2 MW steam turbogenerator was added to the project (18.2 MM\$) (3). Capital costs associated with capturing CO₂ from flue gas were adapted assuming amine-based absorption and stripping (including compression) as reported in Kim et al., (2012) (56). The direct cost estimate was assumed to scale linearly (4.4-fold to 35 MM\$). Operating costs associated with capturing CO₂ from flue gas were adapted from Geissler and Maravelias (2021) (46). Heat required to capture flue gas was provided by natural gas at a rate of 325 kg/hr. Electricity required to capture flue gas totaled 9.0 MWh and was deducted from the electricity produced onsite. The steam turbogenerator loop reported in Humbird et al., 2011 generates 41.37 MWh electricity, but also includes extracting steam at high-pressure (12%) for thermochemical pretreatment and at low-pressure (35%) for distillation (3). Considering ethanol throughput is nearly equal, distillation duty should remain similar while the generated electricity was adjusted to 47.0 MWh to compensate for absence of high-pressure steam extraction. Exported electricity revenue was determined assuming a selling price of 0.0681 \$/kWh (EIA, 2019 US total average). Solid residue combustion was adapted from Humbird et al., (2011), which produced flue gas at 20% CO₂ by mass (3). Flue gas CO₂ capture yield was assumed to equal 85% (56), generating approximately 0.524-million-ton CO₂ per year.

Economic Analysis

Project economics were determined using the financial assumptions in Humbird et al. (2011), including 40% equity, a 10-year loan at 8% interest terms, and nth plant assumptions. Minimum ethanol selling price (MESP) was determined using a 10% discount rate over a 30-year project lifetime. A 7-year MACRS (modified accelerated cost recovery system) depreciation schedule was assumed for capital investment. Capital and operating costs were estimated for project year 2019, including the corporate tax rate of set at 21%. All scenarios were assumed to have identical indirect costs. For calculating additional direct costs, CO₂ compression and pellet production capital equipment were considered inside battery limits (ISBL).

Corn stover feedstock cost was assumed to equal \$81.37/dry metric ton according to the Herbaceous Feedstock nth-supply state of technology (SOT) report by the Idaho National Laboratory (INL) (57) and reflects preprocessed corn stover delivered to the reactor throat at the biorefinery. Fuel pellet price was determined using data available through the US Energy Information Agency (EIA) (58). The 2019 annual average domestic price for densified biomass fuel was selected for this analysis at \$166/ton. A sensitivity analysis for fuel pellet selling prices towards MESP was included in appendix A.7. The 2019 annual average price for industrial electricity was \$0.0681/kWh, (EIA) (59). No market value was assigned to excess biogas in scenario I that was not utilized or upgraded. A selling price of \$50 per ton of CO₂ was chosen in light of the supply chain logistics not included in this analysis (transportation, injection, monitoring) (25,37,60–62). The US tax credit for carbon sequestration was recently (2022) raised from \$50 to \$85 per ton CO₂ for geologic storage (63).

The D3 RIN credit was selected as the basis for the RNG selling price in this analysis and was averaged using data provided by the Environmental Protection Agency (EPA) for all D3 transfers in 2019 (64) (data also available in appendix B). The D3 RIN credit value equaled \$1.35/gallon ethanol, or \$17.70/MMBtu, while the natural gas selling price in 2019 averaged 2.56\$/MMBtu (Henry Hub natural gas spot price) (65) underscoring the possible advantages to coproducing RNG, as the credit is almost 7-fold higher than the fossil fuel equivalent. Data on D3 RIN pricing over the last decade provided by the EPA is also included in appendix B.

Levelized costs for CO₂ capture were calculated based on CO₂ compressor capital cost and electricity demand. Remaining operation and maintenance costs were assumed to be covered by existing ISBL fixed costs and labor and are already included in this analysis (3,30). To annualize capital expenses for levelized cost calculations, a 15% factor was applied to the total purchase cost. Lastly, the CO₂ levelized costs do not factor in the revenue of RNG, ethanol, or fuel pellets. Calculations for levelized costs are presented in appendix A.6.

GHG Accounting

Relative biorefinery GHG emissions were determined focusing on the cellulosic ethanol manufacturing facility and MJ ethanol as the comparative metric (g CO₂ equivalent per MJ ethanol). Simulated mass and energy balances were used to determine biorefinery greenhouse gas emissions. Emissions related to the corn stover supply chain were estimated at 59.92 kg CO₂eq per metric ton (GREET® 2022 v1.3.0.13991) (66,67). Life-cycle emissions related to ethanol/coproduct transport and distribution were not considered in this analysis. Geologic CO₂ storage and avoided fossil fuel emissions (AFPE) for products other than ethanol were included in the GHG accounting. The carbon displacement factor for fuel pellets was determined to be 0.61 by dividing the LHV of fuel pellets (16.3 MJ/kg) by the LHV of bituminous coal (29.0 MJ/kg). Thus, for each CO₂ equivalent in fuel pellets utilized (i.e., combusted), 0.61 of CO₂ equivalents related to coal combustion are avoided. A sensitivity analysis for fuel pellet fossil fuel displacement towards net biorefinery GHG reductions was included in appendix A.7. RNG was assumed to have a 1:1 carbon displacement factor with natural gas on a CO₂ equivalent basis. Nutrient inputs to support biological growth were added in the form of corn steep liquor and urea, which were assumed to have carbon intensities equal to 0.935 and 0.878 gCO₂eq/g (GREET® 2022 V1.3.0.13991) (66,67). The carbon emissions related to grid electricity consumption were calculated as 0.417 kg CO₂/kWh using the 2019 national averages for CO₂ emissions related to electricity generation and emissions provided by the US EIA (appendix B) (59).

Results and Discussion

Carbon and Energy Balances

Process design scenarios were analyzed in a stepwise fashion with the later scenarios including features from previous scenarios (appendix A.5). The fate of feedstock carbon and energy is depicted in Figures 2.A and 2.B, respectively. Adjustments considered here did not dramatically affect fractional energy recovery in final fuel products apart from eliminating natural gas in Scenario I. This is

largely attributable to unchanged conversion parameters leading to equal production of ethanol and fuel pellets across all the scenarios.

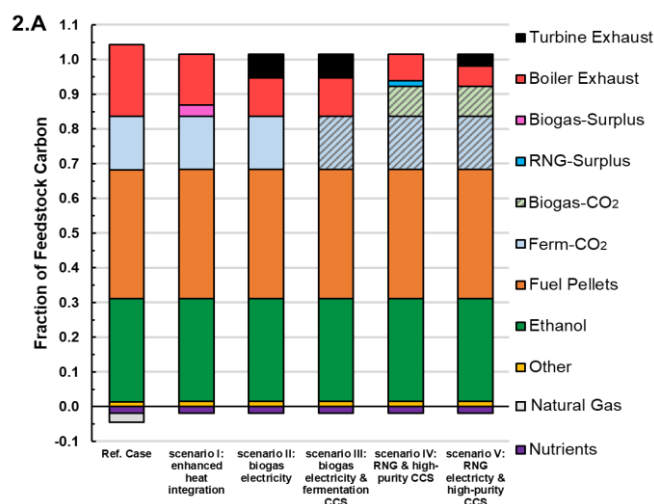


Figure 2.A. Carbon balances represented as terminal fraction of feedstock carbon input. Material Balances generated using ASPEN PLUS process simulations. Dashed bars represent high-purity CO₂ streams purposed for carbon capture and storage.

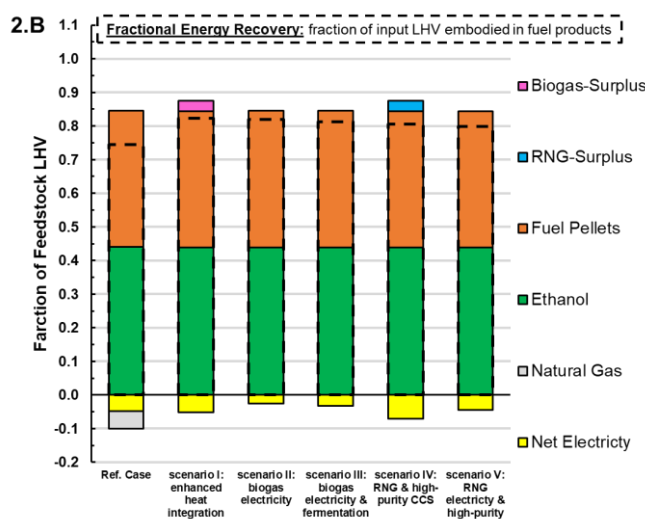


Figure 2.B. Energy balances represented as terminal fraction of feedstock lower heating value (LHV). Fractional energy recovery (black dashed bars) represents the fraction of feedstock energy input embodied in terminal fuel products and is the sum of positive and negative contributions seen above.

In scenario I, enhancing heat recovery completely eliminated natural gas consumption in the reference case (used for process heat) and led to a surplus of biogas available (17.5% of total). Fractional energy recovery, defined by the fraction of input LHV leaving in fuel products, increased by 8% by enhancing heat recovery in scenario I. Similarly, Pourhashem et al. (2013) also found that onsite biogas from stillage can meet steam demands without lignin/solids combustion (68). In scenario II, surplus biogas was used to generate electricity onsite via a gas turbine, with 61% of the biogas fed to the steam boiler and 39% fed to the turbine. Recovering heat from turbine exhaust enables a larger fraction of biogas (39% instead of 17.5%) to be routed towards the turbine for electricity generation. By producing electricity from surplus biogas, externally supplied

(grid) electricity consumption was reduced by 49%, relative to the reference case. In Scenario III, near-pure CO₂ produced by fermentation is compressed in advance of transportation and storage, representing 15.4% of feedstock carbon input. There was a 16.4% increase in total electricity demand for compression of fermentation CO₂, resulting in approximately 7.3 kg CO₂ compressed per kWh consumed. From a GHG perspective, this compares favorably with the current (i.e., 2019) grid carbon intensity 0.417 kg CO₂ per kWh (see methods). In scenario IV, biogas membrane upgrading was included, and the total supply of RNG was split 82.5% & 17.5% between supplying process heat and sold surplus RNG, respectively. This generated an additional fuel stream, surplus RNG, but required 43% more grid electricity consumption than the reference case due to membrane separation and CO₂ capture demands. Biogas membrane separation enabled an additional 8.6% of feedstock carbon to be captured from biogas. Combining the CO₂ streams from fermentation and biogas resulted in nearly a quarter of feedstock carbon (24.0%) available for permanent geologic storage. Of note, this result was obtained without any CO₂ separation from dilute flue streams, i.e., the boiler or turbine exhausts. Lastly, in scenario V, utilizing surplus-RNG onsite to generate electricity via a gas turbine (instead of selling surplus RNG) enabled biogas-CO₂ to be captured while also offsetting grid electricity consumption (Figure 2). Scenario V required roughly the same amount of electricity as the starting reference case while also delivering a significant fraction (i.e., 24.0%) of feedstock carbon input to permanent geologic storage. Regarding uncaptured yet stationary exhaust emissions, in scenario V only 9% of feedstock carbon input is emitted via onsite combustion (Figure 2.A), and the bulk of potential flue gas carbon (37%) is leaving the facility as coproduct fuel pellets.

Capital Investment, Costs, and Revenues

The total capital investment for each scenario is depicted in Figure 3.A. Total capital investment for a 60 million gallon per year (MMgal/yr) facility varied between 280–340 MM\$. These compared favorably with the Humbird et al. (2011) total capital investment estimate of 488 MM\$ (adjusted to 2019\$) for a 61 MMgal/yr facility using a conventional processing paradigm involving thermochemical pretreatment and added fungal cellulase. The gas turbine capacity was approximately 9 MW and estimated at 7.0 MM\$ for scenarios II, III, and V. The capital investment for fermentation-CO₂ compression was 6.7 MM\$ (scenario III) and 8.7 MM\$ for scenarios with additional biogas-CO₂ compression (IV & V). Capital expenses related to biogas upgrading via membrane separation totaled \$17.9 million (scenario IV and V). Generally, the capital investments that enable additional GHG reductions presented throughout this study were small compared to the 285 MM\$ total capital investment required for the reference case.

Product revenue and operating costs for each scenario are depicted in Figure 3.B. Note that ethanol revenue was determined by multiplying ethanol output (equal among all scenarios) by the scenario MESP, which led to different ethanol revenues in each scenario despite all the scenarios having the same profitability, i.e., 30-year project net present value equal to zero assuming a 10% discount rate. As can be observed from Figure 3.B, feedstock dominates operating costs among all the scenarios underscoring its importance to project economics. In Scenario I, elimination of natural

gas consumption led to a small improvement in operating costs and project economics. In scenario II, grid electricity operating costs were split in half by utilizing surplus biogas onsite via gas turbine. Scenario III built on that result, but also included a small coproduct revenue from fermentation CO₂ to CCS. In scenario IV, the coproduct revenue from surplus-RNG and biogas-CO₂ was realized but was largely offset by an 115% increase in electricity operating costs relative to scenario III. When compared to the revenue from ethanol or fuel pellets, the coproduct revenue from either CO₂ or surplus-RNG was roughly an order of magnitude smaller.

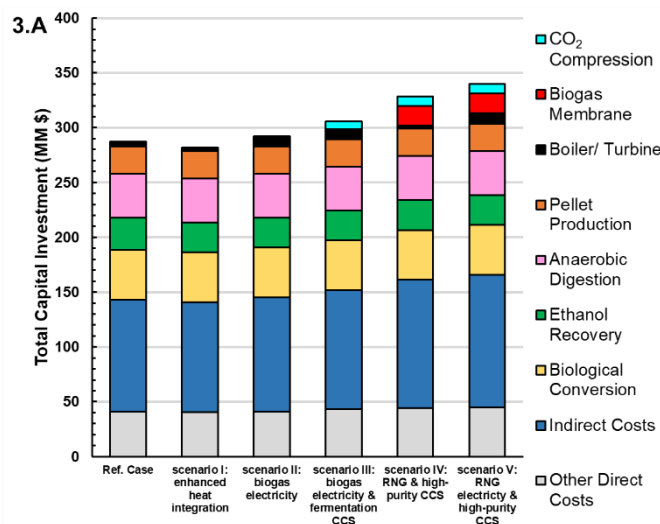


Figure 3.A. Total capital investment. All scenarios generate 60 million gallons per year (MMgal/yr) and process 2,000 dry metric tons of corn stover per day. Capital equipment purchase cost estimation and a summary of total capital investment is available in appendix B.

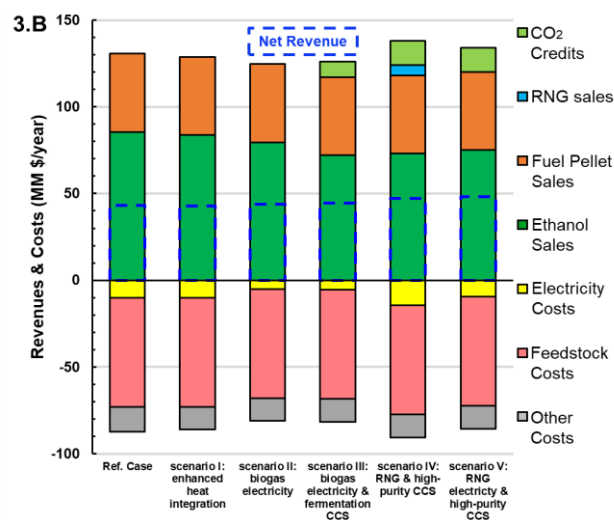


Figure 3.B. Revenues and costs. Minimum ethanol selling prices (MESPs) were used to determine ethanol revenue leading to variable ethanol revenues despite the same throughput (60 MMgal/yr) and profitability. Only the reference case includes natural gas consumption, which is included under the label other costs. Net revenue (dashed blue bars) is equal to revenues minus costs.

The CO₂ levelized cost of capture was estimated to be between \$13.7 and \$14.8/ton CO₂ depending on the scenario (appendix A.6). Levelized costs were lower for scenarios IV and V than III due to capturing additional biogas-CO₂ and economies of scale for compressor capital investment. Levelized costs of capture were

similar to those found in the literature for cases where CCS was selectively applied to high-purity streams (11,25,26). The total levelized cost of carbon abatement, including transportation and storage, would be higher. For comparison, levelized transport costs have been reported in the range of \$5-14/ton CO₂ (11,28,37,60), storage in the range of \$6-24/ton (11,38), and monitoring \$0.1-0.3/ton (62). At a manufacturing-gate assumed selling price of \$50/metric ton, adding high-purity CCS is profitable compared to not doing so.

Scenario Comparisons: GHG reductions and MESP

Relative GHG reductions and MESP for each scenario are presented in Figure 4. Generally, all process design scenarios presented here lowered the MESP and improved GHG reductions relative to the reference case. Many of the GHG reduction measures considered here impart only minor increases in total capital investment (Figure 3.A) and no changes in ethanol and fuel pellet production (Figure 2.A and 2.B). Avoided fossil fuel emissions (AFFE) afforded by fuel pellets were equal in all scenarios presented here and was determined assuming coal displacement (see methods). Later scenarios, with overall larger negative emissions, were less sensitive towards fuel pellet AFFE (appendix A.7). Despite additional capital investment, decreasing MESP (\$1.43, \$1.39, \$1.34, \$1.23, \$1.27, \$1.31 per gallon ethanol, respectively) indicate that the process design modifications would improve project economic outcomes overall. It should be noted that MESP depends on financial assumptions, production scale, and project schedule, and variables assumed here align with the *n*th plant analysis as specified by NREL (Humbird et al., 2011). Estimated MESP here range from \$1.23 to \$1.43 per gallon ethanol,

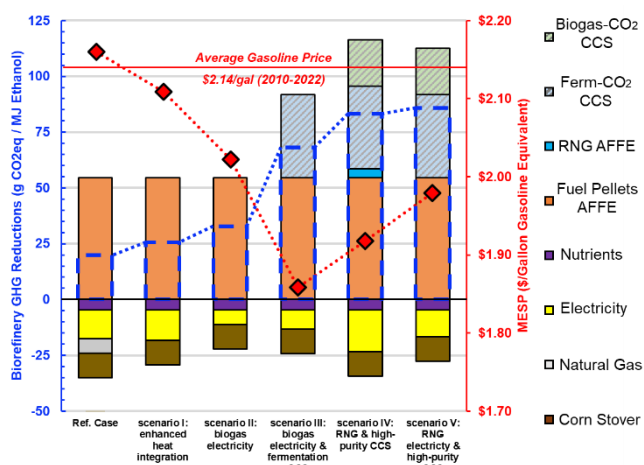


Figure 4. Greenhouse gas (GHG) reductions and minimum ethanol selling prices (MESP) for each scenario. AFFE: avoided fossil fuel emissions. GHG emissions determined on a gCO₂ equivalent per MJ ethanol basis for a 60 million gallon per year facility. MESP determined on gallon gasoline equivalent (GGE) basis. Average wholesale gasoline price (solid red line) reported by the EIA between 2010-2022 equaled \$2.14/gal with a single standard deviation of \$0.59. Minimum ethanol selling price (MESP) (red bars) was determined using the same financial assumptions as Humbird et al. (2011) for a 30-year project with a 10% discount factor. Net biorefinery GHG reductions (dashed blue bars) were determined by summing positive and negative contributions presented here.

which is in the lower end of estimates previously reported for corn stover ethanol (especially compared to studies from the past decade) (appendix A.1). Inclusion of high-purity CCS resulted in lower MESP values than without and enabled cost-competitive ethanol on a gasoline equivalent basis. Over the last fifteen years, the average

wholesale selling price of gasoline has equaled \$2.14/gal gasoline (+/- 0.59 \$/gal, i.e., one standard deviation) (EIA data) whereas ethanol MESP's reported here range between \$1.86 and \$2.17 per gallon of gasoline equivalent (GGE) (appendix B), underscoring the cost-competitiveness with wholesale gasoline.

Eliminating natural gas consumption in scenario I led to a marginal improvement in GHG reductions and leaves externally purchased (i.e., grid) electricity as the largest remaining fossil fuel input. Scenario II builds on this result, utilizing surplus biogas via gas turbine and cutting electricity imports nearly in half. Possible GHG benefits realized by minimizing grid electricity may be transient, i.e., not reflective of future low-carbon grid technology (69), while those of CCS would persist in, and indeed help enable, a net-zero carbon economy. Compared to scenario II, deploying CCS for fermentation CO₂ in scenario III resulted in a 2.1-fold improvement in the net GHG emission reductions (an additional -35 gCO₂eq/MJ ethanol) and lowered MESP from \$2.03 to \$1.86 per GGE. Scenario IV introduced biogas upgrading via membrane separation to sell surplus RNG which required additional electricity and sacrificed any onsite electricity generation via RNG-turbine. Ultimately, only 17.5% of RNG is sold (i.e., the surplus, corresponding to 1.6% of feedstock carbon input) and thus the much larger contribution to GHG emission reductions is the biogas-CO₂ byproduct stream, corresponding to 8.6% of feedstock carbon input. Scenario V displaced more grid electricity CO₂ equivalents than RNG coproduct sales in scenario IV, yielding the highest GHG emission reduction among the scenarios simulated thus far. The reference scenario's net biorefinery GHG emission reduction was estimated at -19.5 gCO₂eq/MJ ethanol and -84.8 gCO₂eq/MJ for Scenario V, thus, the cumulative impact of the changes described throughout this study increased the carbon abatement by 4.3-fold while simultaneously lowering the minimum ethanol selling price.

Up to this point, the analysis has primarily focused on the energy and economic efficiencies related to capturing high-purity CO₂ streams at the biorefinery. However, it is also possible to imagine a total CCS approach which would also capture more dilute flue gas CO₂. The net biorefinery GHG reductions in a total-CCS approach nearly doubled to -157 gCO₂eq/MJ ethanol (Figure 5). However, this increased the capital investment from 322 to 445 MM\$ while reducing total revenue from 137 to 118 MM\$ per year. Despite exporting 9 MW electricity to the grid, the minimum ethanol selling price was increased 1.4-fold (1.98 to 2.74 \$/GGE, respectively). This result is consistent with the prior study, Lynd et al. (2017), that demonstrated lower operational costs and project investment based on fuel pellet coproduction rather than onsite electricity production (20). Notably, the trade-off between economics and GHG reductions is not observed when capturing only high-purity streams.

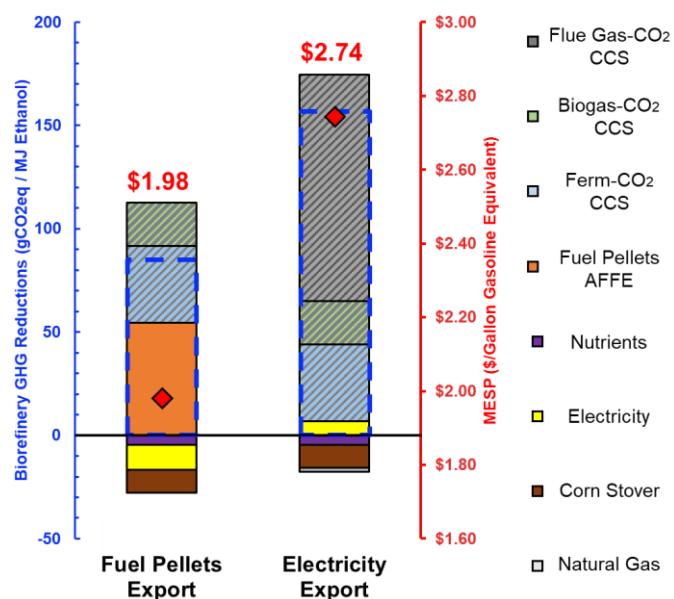


Figure 5. Greenhouse gas (GHG) reductions and minimum ethanol selling prices for coproduction of fuel pellets or electricity. AFFE: avoided fossil fuel emissions. GHG emissions determined on a gCO_2eq per gallon gasoline equivalent (GGE) basis for a 60 million gallon per year facility. Scenario V is duplicated from Figure 4 with no changes titled fuel pellets export. Net biorefinery GHG reductions (dashed blue bars) were determined by summing positive and negative contributions presented here.

All scenarios considered thus far, with the exception of electricity export in Figure 5, take a credit for AFFE from fuel pellet conversion to electricity, assuming coal displacement. Figure 6 considers the mitigation impact of capturing CO_2 from fuel pellet combustion stack gas assuming either contemporary (2019) carbon intensity and AFFE or a futuristic zero-carbon intensity scenario implying no fossil fuel displacement (AFFE) or carbon emissions associated with imported electricity or RNG. For the contemporary case, $-170 \text{ gCO}_2\text{eq}/\text{MJ}$ ethanol net mitigation is achieved from flue gas capture (80% originating from fuel pellets), fuel pellet AFFE, fermentation CO_2 capture, and biogas CO_2 capture, ranked in that order. Subtracting

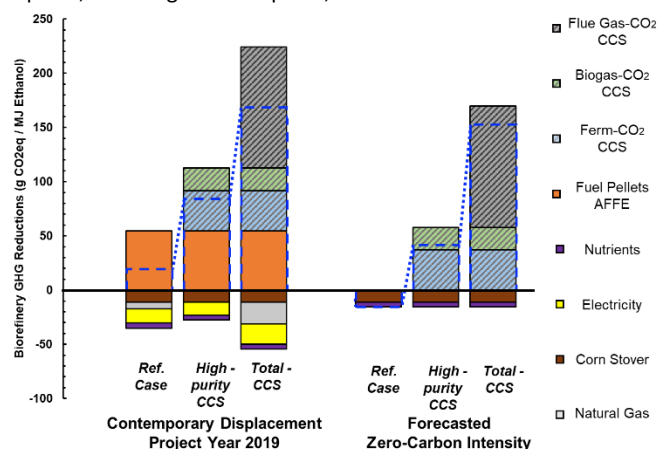


Figure 6. Net GHG reductions in a total-CCS configuration for both a contemporary and futuristic scenario. AFFE: avoided fossil fuel emissions. GHG emissions determined on a per MJ ethanol basis for a 60 million gallon per year facility. The reference case is duplicated from Figure 4 with no changes, and scenario V is duplicated from Figure 4 with no changes titled High-purity CCS here. In the total - CCS scenario, heat and power demands associated with flue gas capture were adapted from the electricity export scenario in Figure 5. Net biorefinery GHG reductions (dashed blue bars) were determined by summing positive and negative contributions presented here.

emissions from electricity and RNG assuming zero carbon intensity achieves net mitigation of $-154 \text{ gCO}_2\text{eq}/\text{MJ}$ ethanol.

In summary, it would be possible to economically recover 24% of feedstock carbon as high purity gas (fermentation off-gas and separated biogas), and an additional 46% from solids and biogas combustion for a total of 70% of feedstock carbon capturable. These streams correspond to 0.276, 0.105, and 0.524 million tons of CO_2 annually available, respectively, all originating from a 60 MMgal/yr facility. These results demonstrate the potential for improving GHG mitigation benefits as cellulosic biofuel technology matures.

Conclusions

This study offers an updated technoeconomic evaluation of corn stover conversion to ethanol via C-CBP at a scale of 60 million gallon per year. Compared to the reference case (Lynd et al., 2017), each of the revised scenarios presented here enables additional GHG emission reductions while simultaneously decreasing the MESP. Enhanced heat recovery eliminated natural gas input and generated surplus biogas. Results indicate that carbon capture and storage (CCS) from fermentation sources is a direct and cost-effective (MESP: \$1.23/gal) pathway to enabling negative carbon flux (15.4% of feedstock carbon input) and significant GHG emission reductions (an additional $-35 \text{ gCO}_2\text{eq}/\text{MJ}$ ethanol). In another scenario (IV), Biogas membrane separation enables selling surplus RNG and captures an additional 8.6% of feedstock carbon input, or 24% combined. In the final scenario (V), GHG reductions are 4.3-fold higher while the MESP is nearly 10% lower than the starting reference case for an 18% increase in total capital investment. These results underscore the role cellulosic ethanol can play in realizing negative carbon emissions at the biorefinery. The levelized cost of capture for fermentation CO_2 , both with and without biogas CO_2 , was \$13.7 and \$14.8/ton, respectively, both of which compare favorably with the existing price incentives for geologic storage (\$85/ton overall). Overall, our analysis suggests that 1) a corn-stover-to-ethanol facility can be self-sufficient in process heat without onsite combustion of solid process residues, 2) compared to wholesale gasoline, the C-CBP platform offers cost-competitive cellulosic ethanol with MESP's ranging between \$1.86 and \$2.17/GGE, 3) capturing CO_2 from fermentation was a relatively straightforward path to enabling negative carbon flux (plus coproduct revenue) and when coupled with biogas upgrading, enables capture of 24% feedstock carbon input without using dilute flue streams, and 4) a total-CCS approach would enable recovering 70% of feedstock carbon from stationary sources.

Author Contributions

Matthew R. Kubis: Conceptualization, Methodology, Investigation, Formal analysis, Writing – Original Draft, Writing – Review & Editing. Lee R. Lynd: Conceptualization, Writing – Review & Editing, Supervision, Funding acquisition.

Conflicts of interest

MRK, none. LRL is an equity holder in a cellulosic biofuel company.

Acknowledgements

The authors acknowledge Tom L. Richard, Dan L. Sanchez, and Mark S. Laser for useful discussions, and the Center for Bioenergy Innovation, a US Department of Energy Bioenergy Research Center supported by the Office of Biological and Environmental Research in the DOE Office of Science, for financial support.

Notes and references

- International Energy Agency. Technology Roadmap: Delivering Sustainable Bioenergy. Paris; 2017.
- Wang M, Han J, Dunn JB, Cai H, Elgowainy A. Well-to-wheels energy use and greenhouse gas emissions of ethanol from corn, sugarcane and cellulosic biomass for US use. Efficiency and Sustainability in Biofuel Production: Environmental and Land-Use Research. 2012;7(045905).
- Humbird D, Davis R, Tao L, Kinchin C, Hsu D, Aden A, et al. Process Design and Economics for Biochemical Conversion of Lignocellulosic Biomass to Ethanol: Dilute-Acid Pretreatment and Enzymatic Hydrolysis of Corn Stover. Golden, CO; 2011 May.
- Huang HJ, Ramaswamy S, Al-Dajani W, Tschirner U, Cairncross RA. Effect of biomass species and plant size on cellulosic ethanol: A comparative process and economic analysis. Biomass Bioenergy. 2009 Feb;33(2):234–46.
- U.S. Department of Energy. 2016 Billion-Ton Report: Advancing Domestic Resources for a Thriving Bioeconomy. Oak Ridge, TN; 2016 Jul.
- Tao L, Markham JN, Haq Z, Bidy MJ. Techno-economic analysis for upgrading the biomass-derived ethanol-to-jet blendstocks. Green Chemistry. 2017;19(4):1082–101.
- Hannon JR, Lynd LR, Andrade O, Benavides PT, Beckham GT, Bidy MJ, et al. Technoeconomic and life-cycle analysis of single-step catalytic conversion of wet ethanol into fungible fuel blendstocks. PNAS. 2019; 117(23):12576–83.
- Lynd LR, Beckham GT, Guss AM, Jayakody LN, Karp EM, Maranas C, et al. Toward low-cost biological and hybrid biological/catalytic conversion of cellulosic biomass to fuels†. Vol. 15, Energy and Environmental Science. Royal Society of Chemistry; 2022. p. 938–90.
- McKechnie J, Pourbafrani M, Saville BA, MacLean HL. Exploring impacts of process technology development and regional factors on life cycle greenhouse gas emissions of corn stover ethanol. Renew Energy. 2015 Apr 1;76:726–34.
- Zhao L, Ou X, Chang S. Life-cycle greenhouse gas emission and energy use of bioethanol produced from corn stover in China: Current perspectives and future perspectives. Energy. 2016 Nov 15;115:303–13.
- Kim S, Zhang X, Reddy AD, Dale BE, Thelen KD, Jones CD, et al. Carbon-Negative Biofuel Production. Environ Sci Technol. 2020 Sep 1;54(17):10797–807.
- Qin Z, Canter CE, Dunn JB, Mueller S, Kwon H, Han J, et al. Land management change greatly impacts biofuels' greenhouse gas emissions. GCB Bioenergy. 2018 Jun 1;10(6):370–81.
- Wooley R, Ruth M, Sheehan J, Ibsen K, Majdeski H, Galvez A. Lignocellulosic Biomass to Ethanol Process Design and Economics Utilizing Co-Current Dilute Acid Prehydrolysis and Enzymatic Hydrolysis Current and Futuristic Scenarios. Golden, CO; 1999 Jul.
- Mcaloon A, Taylor F, Yee W, Ibsen K, Wooley R. Determining the Cost of Producing Ethanol from Corn Starch and Lignocellulosic Feedstocks. Golden, CO; 2000 Oct.
- Aden A, Ruth M, Ibsen K, Jechura J, Neeves K, Sheehan J, et al. Lignocellulosic Biomass to Ethanol Process Design and Economics Utilizing Co-Current Dilute Acid Prehydrolysis and Enzymatic Hydrolysis for Corn Stover. Golden, CO; 2002 Jun.
- Kazi KF, Fortman J, Anex R, Kothandaraman G, Hsu D, Aden A, et al. Techno-Economic Analysis of Biochemical Scenarios for Production of Cellulosic Ethanol. Golden, CO; 2007.
- Lynd LR. The grand challenge of cellulosic biofuels. Vol. 35, Nature Biotechnology. Nature Publishing Group; 2017. p. 912–5.
- Salles-Filho SLM, Castro PFD de, Bin A, Edquist C, Ferro AFP, Corder S. Perspectives for the Brazilian bioethanol sector: The innovation driver. Energy Policy. 2017;108:70–7.
- Salles-Filho SLM, Cortez LAB, Silveria JMFJ, Trindade SC, Fonseca MGD (Eds.). Global Bioethanol: Evolution, Risks, and Uncertainties. London, UK: Academic Press; 2016.
- Lynd LR, Liang X, Bidy MJ, Allee A, Cai H, Foust T, et al. Cellulosic ethanol: status and innovation. Vol. 45, Current Opinion in Biotechnology. Elsevier Ltd; 2017. p. 202–11.
- Lam CH, Das S, Erickson NC, Hyzer CD, Garedew M, Anderson JE, et al. Towards sustainable hydrocarbon fuels with biomass fast pyrolysis oil and electrocatalytic upgrading. Sustain Energy Fuels. 2017;1(2):258–66.
- Das S, Anderson JE, De Kleine R, Wallington TJ, Jackson JE, Saffron CM. Comparative life cycle assessment of corn stover conversion by decentralized biomass pyrolysis-

ARTICLE

Journal Name

- electrocatalytic hydrogenation versus ethanol fermentation. *Sustain Energy Fuels*. 2022 Dec 21;7(3):797–811.
23. Sandalow D, Aines R, Friedmann J, McCormick C, Sanchez DL. Biomass Carbon Removal and Storage (BiCRS) Roadmap. Livermore, CA; 2021 Jan.
24. Rosa L, Sanchez DL, Mazzotti M. Assessment of carbon dioxide removal potential: Via BECCS in a carbon-neutral Europe. *Energy Environ Sci*. 2021 May 1;14(5):3086–97.
25. Yang M, Baral NR, Anastasopoulou A, Breunig HM, Scown CD. Cost and Life-Cycle Greenhouse Gas Implications of Integrating Biogas Upgrading and Carbon Capture Technologies in Cellulosic Biorefineries. *Environ Sci Technol*. 2020 Oct 20;54(20):12810–9.
26. Geissler CH, Maravelias CT. Economic, energetic, and environmental analysis of lignocellulosic biorefineries with carbon capture. *Appl Energy*. 2021 Nov 15;302.
27. Gelfand I, Hamilton SK, Kravchenko AN, Jackson RD, Thelen KD, Robertson GP. Empirical Evidence for the Potential Climate Benefits of Decarbonizing Light Vehicle Transport in the U.S. With Bioenergy from Purpose-Grown Biomass with and without BECCS. *Environ Sci Technol*. 2020 Mar 3;54(5):2961–74.
28. Psarras PC, Comello S, Bains P, Charoensawadpong P, Reichelstein S, Wilcox J. Carbon Capture and Utilization in the Industrial Sector. *Environ Sci Technol*. 2017 Oct 3;51(19):11440–9.
29. International Energy Agency. Technology Roadmap: Carbon Capture and Storage. Paris; 2013.
30. Herron S, Zoelle A, Summers WM. Cost of Capturing CO₂ from Industrial Sources [Internet]. Pittsburgh, PA; 2014.
31. Leeson D, Mac Dowell N, Shah N, Petit C, Fennell PS. A Techno-economic analysis and systematic review of carbon capture and storage (CCS) applied to the iron and steel, cement, oil refining and pulp and paper industries, as well as other high purity sources. *International Journal of Greenhouse Gas Control*. 2017;61:71–84.
32. Yun S, Oh SY, Kim JK. Techno-economic assessment of absorption-based CO₂ capture process based on novel solvent for coal-fired power plant. *Appl Energy*. 2020 Jun 15;268.
33. James R, Zoelle A, Keairns D, Turner M, Woods M, Kuehn N. Cost and Performance Baseline for Fossil Energy Plants Volume 1: Bituminous Coal and Natural Gas to Electricity. 2019.
34. Xu Y, Isom L, Hanna MA. Adding value to carbon dioxide from ethanol fermentations. Vol. 101, *Bioresource Technology*. 2010. p. 3311–9.
35. Deng L, Hägg MB. Techno-economic evaluation of biogas upgrading process using CO₂ facilitated transport membrane. *International Journal of Greenhouse Gas Control*. 2010;4(4):638–46.
36. Lan W, Chen G, Zhu X, Wang X, Liu C, Xu B. Biomass gasification-gas turbine combustion for power generation system model based on ASPEN PLUS. *Science of the Total Environment*. 2018 Jul 1;628–629:1278–86.
37. Sanchez DL, Johnson N, McCoy ST, Turner PA, Mach KJ. Near-term deployment of carbon capture and sequestration from biorefineries in the United States. *Proc Natl Acad Sci U S A*. 2018 May 8;115(19):4875–80.
38. Baker SE, Stolaroff JK, Peridas G, Pang SH, Goldstein HM, Lucci FR, et al. Getting to Neutral Options for Negative Carbon Emissions in California. Livermore, CA; 2020.
39. Sgouridis S, Carbajales-Dale M, Csala D, Chiesa M, Bardi U. Comparative net energy analysis of renewable electricity and carbon capture and storage. *Nat Energy*. 2019 Jun 1;4(6):456–65.
40. Leeson D, Mac Dowell N, Shah N, Petit C, Fennell PS. A Techno-economic analysis and systematic review of carbon capture and storage (CCS) applied to the iron and steel, cement, oil refining and pulp and paper industries, as well as other high purity sources. *International Journal of Greenhouse Gas Control*. 2017;61:71–84.
41. Laude A, Ricci O, Bureau G, Royer-Adnot J, Fabbri A. CO₂ capture and storage from a bioethanol plant: Carbon and energy footprint and economic assessment. *International Journal of Greenhouse Gas Control*. 2011;5(5):1220–31.
42. Lee U, Kwon H, Wu M, Wang M. Retrospective analysis of the U.S. corn ethanol industry for 2005–2019: implications for greenhouse gas emission reductions. *Biofuels, Bioproducts and Biorefining*. 2021 Sep 1;15(5):1318–31.
43. Xu H, Lee U, Wang M. Life-cycle greenhouse gas emissions reduction potential for corn ethanol refining in the USA. *Biofuels, Bioproducts and Biorefining*. 2022 May 1;16(3):671–81.
44. Lee U, R Hawkins T, Yoo E, Wang M, Huang Z, Tao L. Using waste CO₂ from corn ethanol biorefineries for additional ethanol production: life-cycle analysis. *Biofuels, Bioproducts and Biorefining*. 2021 Mar 1;15(2):468–80.

Journal Name

ARTICLE

45. Finley RJ. An Overview of the Illinois Basin - Decatur Project. *Greenhouse Gases: Science and Technology*. 2014;2(5):571–9.
46. Geissler CH, Maravelias CT. Economic, energetic, and environmental analysis of lignocellulosic biorefineries with carbon capture. *Appl Energy*. 2021 Nov 15;302.
47. Kim S, Zhang X, Reddy AD, Dale BE, Thelen KD, Jones CD, et al. Carbon-Negative Biofuel Production. *Environ Sci Technol*. 2020 Sep 1;54(17):10797–807.
48. Yang M, Baral NR, Anastasopoulou A, Breunig HM, Scown CD. Cost and Life-Cycle Greenhouse Gas Implications of Integrating Biogas Upgrading and Carbon Capture Technologies in Cellulosic Biorefineries. *Environ Sci Technol*. 2020 Oct 20;54(20):12810–9.
49. Walsh JL, Ross CC, Smith MS, Harper SR. Utilization of Biogas. Vol. 20, *Biomass*. 1989.
50. Kang JY, Kang DW, Kim TS, Hur KB. Comparative economic analysis of gas turbine-based power generation and combined heat and power systems using biogas fuel. *Energy*. 2014 Apr 1;67:309–18.
51. Kang DW, Kim TS, Hur KB, Park JK. The effect of firing biogas on the performance and operating characteristics of simple and recuperative cycle gas turbine combined heat and power systems. *Appl Energy*. 2012;93:215–28.
52. Liu Z, Karimi IA. Simulating combined cycle gas turbine power plants in Aspen HYSYS. *Energy Convers Manag*. 2018 Sep 1;171:1213–25.
53. Niu M, Xie J, Liang S, Liu L, Wang L, Peng Y. Simulation of a new biomass integrated gasification combined cycle (BIGCC) power generation system using Aspen Plus: Performance analysis and energetic assessment. *Int J Hydrogen Energy*. 2021 Jun 23;46(43):22356–67.
54. Abatzoglou N, Boivin S. A review of biogas purification processes. Vol. 3, *Biofuels, Bioproducts and Biorefining*. 2009. p. 42–71.
55. Bhattacharyya D, Turton R, Zitney SE. Steady-state simulation and optimization of an integrated gasification combined cycle power plant with CO₂ capture. *Ind Eng Chem Res*. 2011 Feb 2;50(3):1674–90.
56. Kim J, Johnson TA, Miller JE, Stechel EB, Maravelias CT. Fuel production from CO₂ using solar-thermal energy: System level analysis. *Energy Environ Sci*. 2012 Sep;5(9):8417–29.
57. Lin Y, Sadekuzzaman Roni M, Thompson DN, Hartley DS, Griffel M, Cai H. *Herbaceous Feedstock 2020 State of Technology Report*. Idaho Falls, ID; 2020.
58. U.S. Energy Information Agency. Monthly Densified Biomass Fuel Report Form EIA-63C. 2019. Available from: https://www.eia.gov/biofuels/biomass/?year=2019&month=12#table_data
59. U.S. Energy Information Agency. Electricity Data Form EIA-923 Power Plant Operations Report. 2019. Available from: <https://www.eia.gov/electricity/data/state/>
60. Mccollum DL, Ogden JM. *Techno-Economic Models for Carbon Dioxide Compression, Transport, and Storage & Correlations for Estimating Carbon Dioxide Density and Viscosity*. Davis, CA; 2006. Available from: <https://escholarship.org/uc/item/1zg00532>
61. Bock B, Rhudy R, Herzog H, Klett M, Davison J, de La Torre Ugarte DG. *Economic Evaluation of CO₂ Storage and Sink Enhancement Options*. 2003. Available from: <https://www.osti.gov/biblio/826435>
62. Metz B, Davidson O, Connick H, Loos M, Meyer L. *CARBON DIOXIDE CAPTURE AND STORAGE [Internet]*. New York, NY; 2005.
63. U.S. Internal Revenue Code. Title 26 U.S. Code § section 45Q: Credit for carbon oxide sequestration. 2022.
64. U.S. Environmental Protection Agency. RIN Trades and Price Information. 2019. Available from: <https://www.epa.gov/fuels-registration-reporting-and-compliance-help/rin-trades-and-price-information>
65. U.S. Energy Information Agency. Henry Hub Natural Gas Spot Price. 2019. Available from: <https://www.eia.gov/dnav/ng/hist/rngwhhdA.htm>
66. Lampert D, Cai H, Wang Z, Wu M, Han J, Dunn J, et al. *Development of a Life Cycle Inventory of Water Consumption Associated with the Production of Transportation Fuels*. Argonne, Illinois; 2015 Oct.
67. Wang M, Han J, Dunn JB, Cai H, Elgowainy A. Well-to-wheels energy use and greenhouse gas emissions of ethanol from corn, sugarcane and cellulosic biomass for US use. *Environmental Research Letters*. 2012 Jan 1;
68. Pourhashem G, Adler PR, McAloon AJ, Spatari S. Cost and greenhouse gas emission tradeoffs of alternative uses of lignin for second generation ethanol. *Environmental Research Letters*. 2013;8(2).
69. U.S. Energy Information Agency. Annual Energy Outlook 2022 (AEO2022). 2022. Available from: <https://www.eia.gov/outlooks/aeo/>